

Molecular conformations of jet-cooled 2-methylindan and 2-phenylindan

Abdulhamid Hamza

Received: 27 October 2009 / Accepted: 17 May 2010 / Published online: 11 June 2010
© Springer Science+Business Media, LLC 2010

Abstract The molecular conformations of jet-cooled 2-methylindan (2MI) and 2-phenylindan (2PI) have been studied using resonant-enhanced two-photon ionization spectroscopy in combination with ab initio calculations. Both axial (2MI_{ax}) and equatorial (2MI_{eq}) conformers of 2MI have been observed. A 2MI_{eq}/2MI_{ax} conformer ratio of 2.3 was estimated at 298 K, leading to the energy difference, $\Delta E = E_{2\text{MI}_{\text{ax}}} - E_{2\text{MI}_{\text{eq}}}$, of 0.49 kcal/mol. Ab initio calculations predicted three stable conformers of 2PI: two equatorial conformers (2PI_{eq0} and 2PI_{eq90}), and one axial conformer (2PI_{ax}). Only the axial conformer of 2PI (2PI_{ax}) was experimentally observed. The indan ring of 2PI_{ax} is slightly more planar than the indan rings of the two equatorial conformers of 2PI because of the intramolecular C_{sp²}–H/π interactions in 2PI_{ax}. The equatorial conformers of 2PI relax to the more stable axial conformer because of the high pre-expansion temperature (383 K), and relatively low barrier (1.68 kcal/mol) to axial–equatorial interconversion. The barrier (2.33 kcal/mol) to axial–equatorial interconversion in 2MI is high enough to prevent conformational relaxation at the pre-expansion temperature of 298 K. Intramolecular C–H/π interactions are found to be more important in determining the conformational preference of 2PI than 2MI; this can be attributed to the higher acidity of the C_{sp²}–H bond than that of C_{sp³}–H bond.

Keywords Conformations · Spectroscopy · Ab initio · 2-Methylindan · 2-Phenylindan

Introduction

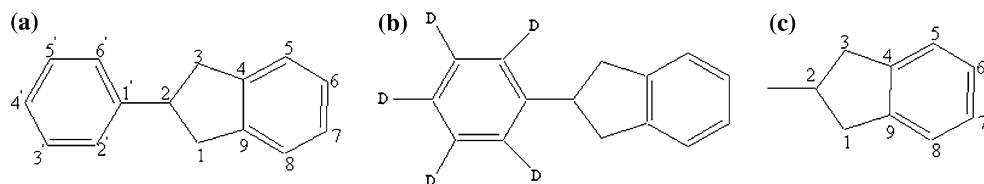
The weak non-bonded interactions of the π electron cloud of aromatic molecules with hydrogen atoms of the C–H, N–H, and O–H bonds have been the subject of several experimental and theoretical investigations [1–7]. These interactions play an important role in determining the conformational preferences of molecules and clusters [1–7]. The interactions are mediated by dispersion and electrostatic forces; the latter are more important in the case of polar N–H and O–H bonds [4]. The C–H/π interactions are dominated by dispersion interactions. The π interactions involving polar N–H and O–H bonds are usually stronger than the C–H/π interactions. For example, the binding energies of benzene–water and benzene–methane clusters are 3.02 kcal/mol and 1.45 kcal/mol, respectively [4].

A red-shift of vibronic transitions is usually associated with C–H/π interactions. Thus, the 6₀¹ bands of benzene–ethylene and benzene–methane clusters are red-shifted by 64 cm⁻¹ and 39 cm⁻¹, respectively, relative to the 6₀¹ band of benzene [1, 8]. Allylbenzene exists predominantly in the eclipsed conformation, which is stabilized by the C–H/π interactions. The electronic origin of the eclipsed conformer of allylbenzene is red-shifted by 121 cm⁻¹ relative to that of the extended conformer [9]. On the other hand, the N–H/π and O–H/π interactions are often associated with the blue-shift of the electronic origins of the molecules and clusters [5]. Thus, the electronic origin of benzene–water cluster is blue-shifted with respect to that of bare benzene by 49 cm⁻¹ [5]. Also, the electronic origin of benzylalcohol is blue-shifted by 50 cm⁻¹ relative to that of toluene [10, 11].

Recently, a large number of conformationally flexible derivatives of indan have been investigated with the primary aim of determining the factors governing the

A. Hamza (✉)
Petroleum Chemistry and Engineering Program,
School of Arts and Sciences, American University of Nigeria,
PMB 2250 Yola, Nigeria
e-mail: abdulhamid.hamza@au.edu.ng

Scheme 1 Structures of **a** 2PI, **b** 2PI-d₅, and **c** 2MI. The puckering angle, p , is defined as C₁–C₂–C₃–C₄. The torsional angle, τ , is defined as C₂–C₁–C₂–H₂



conformational stabilities of organic molecules [2, 3, 6, 7, 12–14]. Only two of the six stable conformers of 1-aminoindan were observed in the supersonic jet experiments of Isozaki et al. [3]. The observed conformers are stabilized by intramolecular N–H/π interactions. The most abundant conformers of 2-aminoindan and 2-indanol are also found to be stabilized by the intramolecular N–H/π and O–H/π interactions, respectively [2, 6]. The electronic origins of the intramolecular N–H/π and O–H/π hydrogen bonded major conformers are blue-shifted relative to the electronic origins of the minor conformers, devoid of intramolecular hydrogen bonding [2, 3, 6, 7, 13].

The main objective of this study was to investigate the role of the C_{sp3}–H/π and C_{sp2}–H/π interactions on the conformational stability of molecules. In order to accomplish this task, the following compounds were synthesized: 2-methylindan (2MI), 2-phenylindan (2PI), and 2-phenylindan-d₅ (2PI-d₅). The structures of these compounds are shown in Scheme 1. Supersonic jet electronic spectra of the synthesized compounds have been recorded using resonant-enhanced two-photon ionization technique, and analyzed with the support of ab initio calculations.

Experimental and computational methods

Synthesis

2-phenylindan was synthesized in three steps. Ethereal solution of phenylmagnesiumbromide (16 mL, 1 M) was slowly added to a solution of 2-indanone (12 mmol in 12 mL of diethylether) at 0 °C. The mixture was stirred for 2 h at room temperature to yield 11 mmol of 2-hydroxyl-2-phenylindan. Bromination of 2-hydroxyl-2-phenylindan (11 mmol) with 7 mmol of PBr₃ in 25 mL of dichloromethane at 20 °C for 2 h yielded 2-bromo-2-phenylindan. A mixture of 2-bromo-2-phenylindan (10 mmol) and magnesium (50 mmol) in methanol (30 mL) was refluxed for 20 h. The reaction mixture was quenched with HCl (12 mL, 3 M). Petroleum ether was then used for the extraction of 2PI. 2PI-d₅ was synthesized following the same procedure as for 2PI. Phenyl magnesiumbromide-d₅ was made by Grignard reaction of bromobenzene-d₅ and magnesium in ether. Ethereal solution of methylmagnesiumbromide (15 mmol, 1 M) was added slowly to a solution of 2-indanone (10 mmol in 15 mL of ether) at

0 °C. The mixture was stirred for 2 h at room temperature to yield 2-hydroxyl-2-methylindan. The latter was brominated with PBr₃ in 20 mL of dichloromethane at 20 °C for 2 h to yield 2-bromo-2-methylindan. 2MI was synthesized by refluxing 2-bromo-2methylindan with magnesium in methanol. The identity of the synthesized compounds was confirmed by GC/MS analysis.

Spectroscopy

The supersonic jet spectrometer used in this study has been described in details elsewhere [15]. Briefly, the spectrometer is composed of two differentially pumped expansion and ionization chambers. The ionization chamber houses the time of flight mass spectrometer; the required high vacuum (2×10^{-7} Torr) in the ionization chamber is achieved by using a liquid nitrogen trap 6-in. diffusion pump. The sample source is located inside the expansion chamber; 9-in. vapor diffusion pump is used to maintain the pressure of about 10^{-3} Torr in the expansion chamber. The sample is heated (to 298 K for 2MI and 383 K for 2PI and 2PI-d₅), and then seeded in a helium carrier gas at a backing pressure of 1–3 atm. The free jet in the expansion chamber is skimmed by a 1-mm skimmer, and the resulting molecular beam in the ionization chamber is perpendicularly crossed by a frequency doubled, Nd:YAG pumped dye laser beam. Molecular ions are formed by sequential absorption of one color resonant and ionizing photons. The molecular ions are then detected and mass analyzed using a time of flight mass spectrometer. Resonant-enhanced two-photon ionization (R2PI) spectra are measured using a boxcar integrator interfaced with a computer.

Ab initio calculations

Ground state optimizations and normal mode analyses of the investigated molecules were initially performed at the Hartree–Fock (HF) level of theory with 6-311G(d,p) basis set. The HF/6-311G(d,p) optimized minima (stable conformers) and maxima (transition states) were then re-optimized using the correlated Møller–Plesset perturbation (MP2) method. It was reported that the MP2 method describes dispersion interactions very well [9]. Since the C–H/π interactions are mostly governed by dispersion interactions and for the sake of brevity, only the results of the MP2/6-311G(d,p) ground state calculations are

reported in this article. The MP2/6-311G(d,p) optimized geometries were used for computing the vertical excitation energies using the time-dependent density functional theory (TDDFT) with B3LYP functional, and the configuration interaction singles (CIS) methods. The CIS method was employed for optimizing the geometries and harmonic frequency calculations of the stable conformers of 2MI and 2PI in their first excited singlet states (S_1). Gaussian03 suite of programs [16] was used for all calculations.

Results and discussion

The cyclopentenyl ring of indan is not planar; therefore, a single substitution at 2-position will lead to two conformers: axial (ax) and equatorial (eq). The puckering angle, p , and the torsional angle, τ , are defined in Scheme 1. Summarized in Table 1 are some of the results of the MP2/6-311G(d,p) ground state optimizations of 2MI and 2PI. All stable conformers of 2MI and 2PI have C_s symmetry. Table 2 lists the computed vertical and adiabatic $S_0 \leftarrow S_1$ excitation energies of all the stable conformers of 2MI and 2PI. $S_0 \leftarrow S_1$ adiabatic excitation energy is the difference in the total energies of the CIS optimized S_1 minimum and the HF optimized S_0 minimum.

Table 1 Summary of the MP2/6-311G(d,p) calculated S_0 data for the stable conformers of 2MI and 2PI

| | 2MI | | 2PI | | |
|--|-------------------|-------------------|-------------------|--------------------|---------------------|
| | 2MI _{ax} | 2MI _{eq} | 2PI _{ax} | 2PI _{eq0} | 2PI _{eq90} |
| $E_{\text{rel}}^{\text{a}}$ (kcal/mol) | 0 | 0.24 | 0 | 0.67 | 1.95 |
| p^{b} (°) | 32.3 | 31.8 | 28.6 | 32.1 | 31.6 |
| τ^{b} (°) | – | – | 0.0 | 0.0 | 89.1 |

^a Relative to the axial conformers

^b The puckering angle, p , and the torsional angle, τ , are defined in Scheme 1

Table 2 Vertical and adiabatic $S_1 \leftarrow S_0$ excitation energies of the stable conformers of 2MI and 2PI

| Vertical $S_1 \leftarrow S_0$ excitation energies using the MP2/6-311G(d,p) S_0 structures | | Adiabatic $S_1 \leftarrow S_0$ excitation energies using the HF/6-311G(d,p) S_0 structures and the CIS/6-311G(d,p) S_1 structures |
|--|-------------------------|---|
| CIS/6-311G(d,p) | TDDFT/B3LYP/6-311G(d,p) | |
| 2MI _{ax} | 48110 | 41848 |
| 2MI _{eq} | 48150 | 41917 |
| 2PI _{ax} | 47787 | 41264 |
| 2PI _{eq0} | 48099 | 41733 |
| 2PI _{eq90} | 48145 | 41846 |
| | | 48009 |
| | | 48030 |
| | | 47822 |
| | | 48015 |
| | | 48063 |

2-Methylindan (2MI)

The optimized structures of the minimum energy conformers of 2MI and the transition state between the two minima are displayed in Scheme 2. The axial conformer (2MI_{ax}) is predicted to be 0.24 kcal/mol more stable than the equatorial conformer (2MI_{eq}) at the MP2/6-311G(d,p) level.

The resonance-enhanced two-photon ionization (R2PI) spectrum of 2MI is displayed in Fig. 1. Two electronic origins are identified at 36903.3 cm⁻¹ and 36924.0 cm⁻¹. The fundamental transitions of the puckering mode appear at 73.6 cm⁻¹ and 75.7 cm⁻¹ from the first and second origins, respectively. These assignments are based on the fact that low frequency vibronic transitions due to the puckering mode have been observed in most of the published electronic spectra of jet-cooled indan and its derivatives [2, 3, 6, 7, 12, 13]. The electronic origins at 36903.3 cm⁻¹ and 36924.0 cm⁻¹ are assigned to the electronic origins of 2MI_{ax} and 2MI_{eq}, respectively, by comparison with the closely related allylbenzene and *n*-propylbenzene [9, 10]. The electronic origins of the eclipsed/gauche conformers (in which the substituent group points toward the aromatic chromophores) of *n*-propylbenzene and allylbenzene are red-shifted relative to those of the extended trans conformers.

As reported in Table 2, the calculated vertical and adiabatic $S_1 \leftarrow S_0$ excitation energies of 2MI_{ax} are less than those of 2MI_{eq}. The CIS/6-311G(d,p) computed puckering frequency in the S_1 state of 2MI_{ax} (78 cm⁻¹) is also less than that of 2MI_{eq} (84 cm⁻¹). Thus, the computed relative $S_1 \leftarrow S_0$ excitation energies and the frequencies of the puckering mode support the assignment of the two electronic origins.

A MI_{eq}/MI_{ax} conformer ratio of 2.3 was estimated by integrating the areas under the origin band of each conformer [6]. The Boltzmann distribution law was then used to estimate their relative energy, $\Delta E = E_{2\text{MI}_{\text{ax}}} - E_{2\text{MI}_{\text{eq}}}$, of 0.49 kcal/mol.

2-Phenylindan

The optimized structures of the minimum energy conformers of 2PI and the transition states between the minima are displayed in Scheme 3.

Two different minima have been found along the phenyl torsional coordinate of the potential energy surface of the equatorial conformer of 2PI at torsional angles, τ , of 0° (2PI_{eq0}) and 90° (2PI_{eq90}). The MP2/6-311G(d,p) relative energy of the 2PI_{eq0} and 2PI_{eq90} conformers is 1.28 kcal/mol in favor of 2PI_{eq0}. The 2PI_{eq90} minimum lies at only 0.06 kcal/mol below the transition state between the 2PI_{eq0} and 2PI_{eq90} (TS_{eq} in Scheme 3).

Scheme 2 Conformational landscape of 2MI

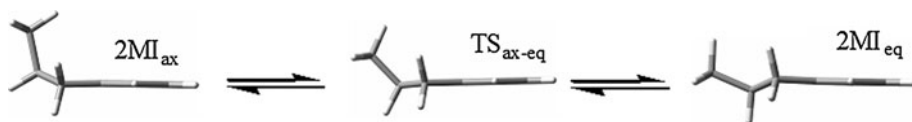
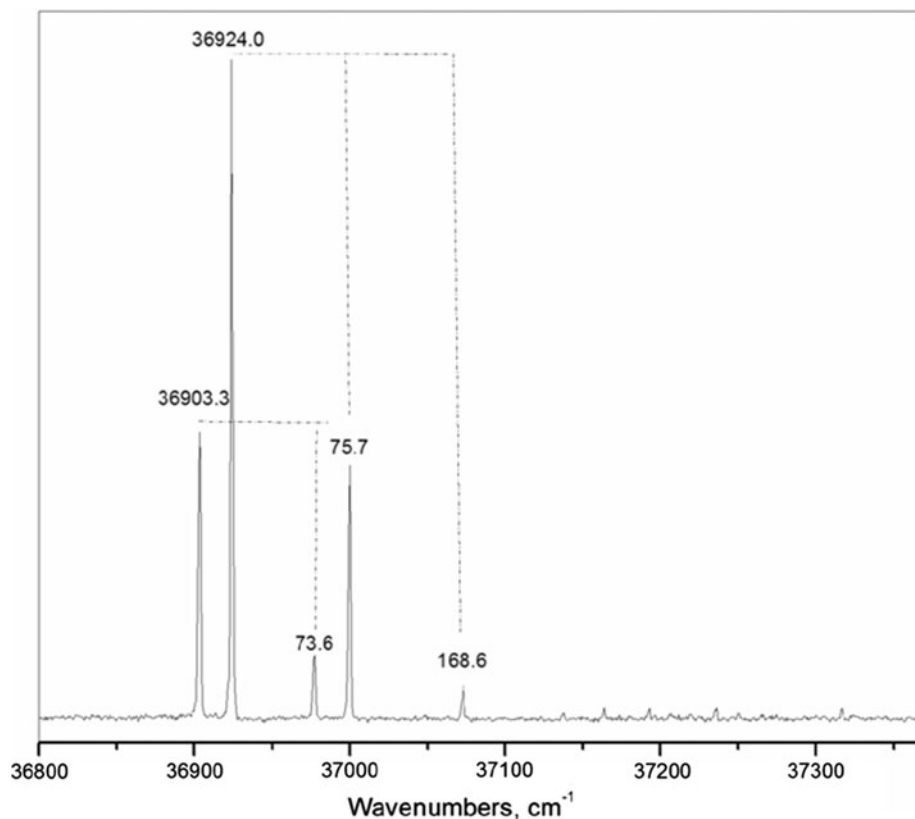


Fig. 1 R2PI spectrum of 2MI



Only one minimum was found along the phenyl torsional coordinate of the axial conformer of 2PI, at $\tau = 0^\circ$. The barrier (TS_{ax} in Scheme 3) to torsional motion is 3.84 kcal/mol. The high barrier in the axial conformer is caused by the repulsive non-bonded interactions between the two ortho hydrogens of the phenyl ring and the two α hydrogens (relative to the phenyl ring) of the indan ring. Here the closest distance between the ortho hydrogens of the phenyl ring and the α hydrogens of the indan ring is 1.95 Å at the MP2/6-311G(d,p) level of theory. It has been reported that the H···H repulsion energy is negligible beyond 2.4 Å but increases to 1 kcal/mol at H···H distance of about 2.0 Å [17].

The main purpose for the synthesis of 2PI-d₅ is to facilitate and support the spectral analysis of 2PI as will be discussed below. It should be noted that both 2PI and 2PI-d₅ have the same symmetry, but different vibrational frequencies because of the higher reduced masses of the vibrational modes of 2PI-d₅. The spectra of 2PI and 2PI-d₅ are displayed in Fig. 2. The frequencies of the electronic origins and the relative frequencies of the major vibronic bands are also shown in Fig. 2. Unlike in the case of 2MI,

there are no obvious vibronic transitions that can be attributed to more than one conformer of 2PI. The first intense peak at 36884.4 cm⁻¹ in the spectrum of 2PI is thus assigned to the electronic origin of 2PI. The most likely candidate for the origin of another conformer of 2PI is the band at 141.6 cm⁻¹ from the assigned origin. However, the corresponding band in the spectrum of 2PI-d₅ has a frequency of 139.9 cm⁻¹. Hence the band at 141.6 cm⁻¹ is not an electronic origin because of the associated isotope effect. Isotopic substitution has very much higher effect on the frequencies of vibronic transitions than on the relative 0_0^0 transition energies of conformers [11].

The observed 0_0^0 transition energies in R2PI spectra correspond to transitions from the vibrationless energy level in the S_0 state to the vibrationless energy level in the S_1 and/or S_2 states. Hence, they cannot be numerically compared with the computed vertical excitation energies at any level of theory. Computation of vertical excitation energies neglects the effect of geometrical relaxation of electronically excited molecules to the vibrationless energy level of the excited electronic states. Ideally, the observed 0_0^0 transition energies should be comparable to the

Scheme 3 Conformational landscape of 2PI

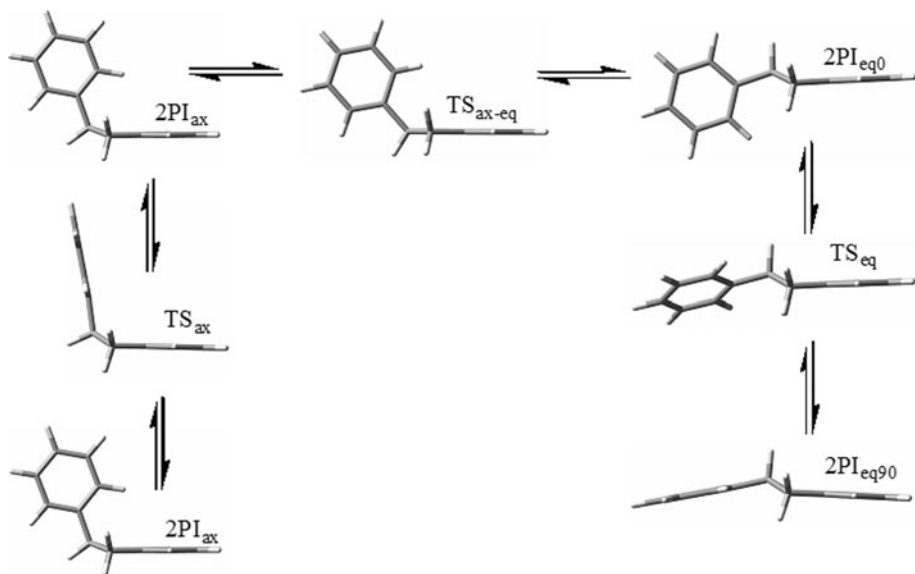
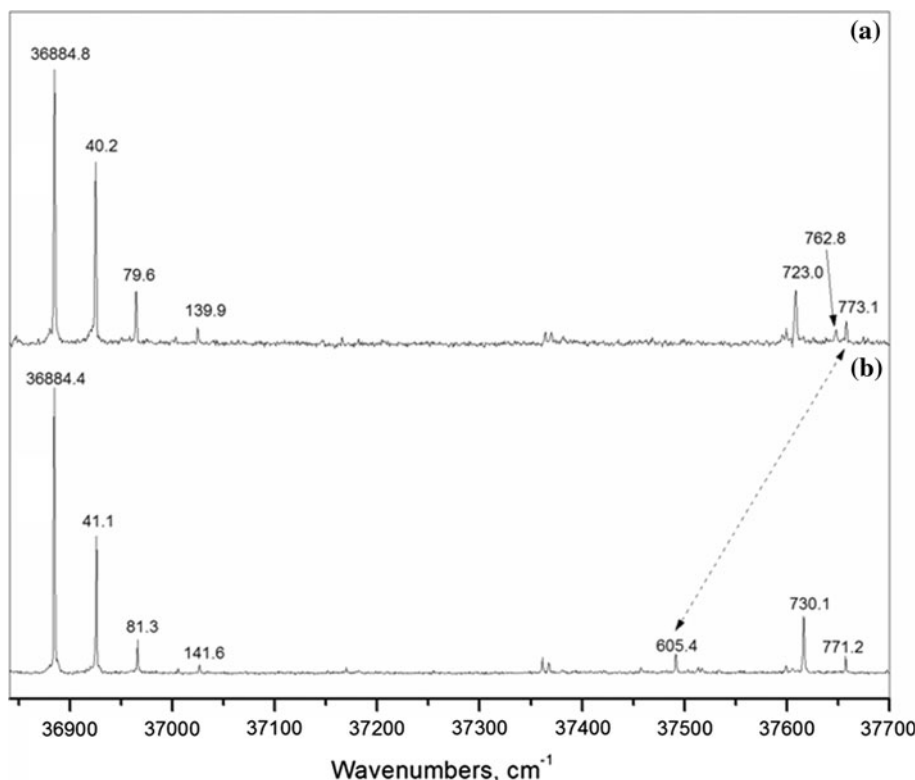


Fig. 2 R2PI spectra of **a** 2PI-d₅ and **b** 2PI

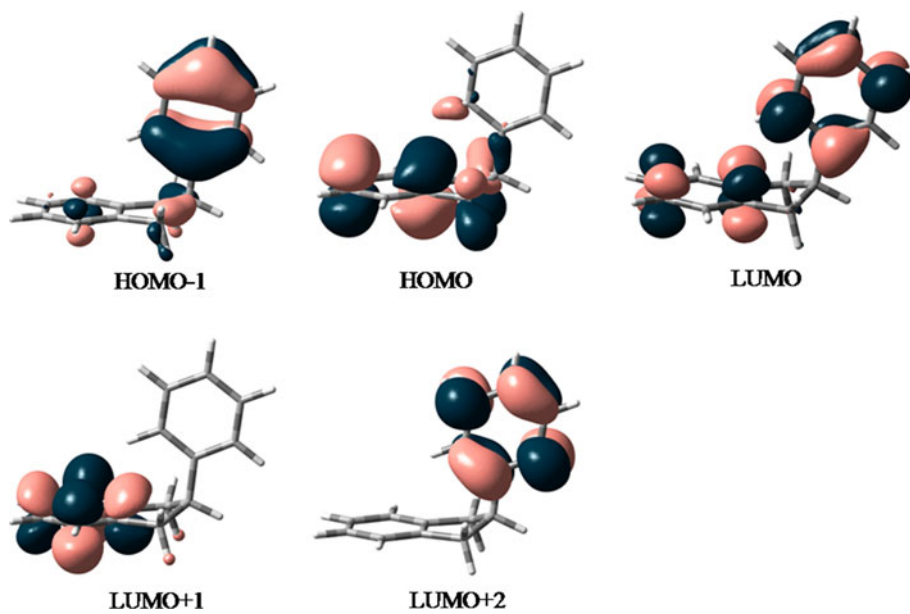


computed adiabatic excitation energies which take relaxation effects into account. TDDFT adiabatic excitation energies cannot be computed using Gaussian03. However, it is well known that the CIS-computed excitation energies are overestimated by about 1 eV due to the inherent approximations in the CIS methodology. Nevertheless, a linear correlation between the CIS-computed adiabatic excitation energies and the observed 0_0^0 transition energies

in a series of aromatic molecules has been found. This permits approximate quantitative comparison of the CIS-computed adiabatic energies and the observed 0_0^0 transition energies in a series of aromatic molecules [19].

The computed $S_1 \leftarrow S_0$ vertical and adiabatic excitation energies of the axial conformer of 2PI (2PI_{ax}) are substantially lower than those of the equatorial conformers (Table 2). The lower excitation energies of the 2PI_{ax}

Fig. 3 Frontier molecular orbitals involved in the $S_1 \leftarrow S_0$ and $S_2 \leftarrow S_0$ transitions of 2PI_{ax}



conformer can be attributed to the lower puckering angles, p , of the axial conformer (Table 1). The greater planarity of the axial conformer is most likely caused by the intramolecular C_{sp2}–H/π interactions. The values of p of the axial and equatorial conformers of 2MI and the equatorial conformers of 2PI are similar. Thus, the calculations suggest that intramolecular C_{sp2}–H/π interactions occur only in the 2PI_{ax} conformer. The slight red-shift of the electronic origin of 2PI with respect to that of the axial conformer of 2MI (2MI_{ax}) can be attributed to the higher intramolecular C_{sp2}–H/π interactions in 2PI_{ax} than intramolecular C_{sp3}–H/π interactions in 2MI_{ax} [1, 8, 9]. Based on these arguments, all vibronic bands in the spectrum of 2PI are due to the most stable 2PI_{ax} conformer. Hence, only the 2PI_{ax} conformer is populated in the supersonic expansion.

The first two CIS/6-311G(d,p) calculated lowest frequency vibrational modes of the 2PI_{ax} conformer in its optimized S_1 state are associated with the puckering and flapping modes, respectively. The calculated frequencies (38 cm^{-1} and 163 cm^{-1}) of these modes are very close to the observed frequencies of 41.1 cm^{-1} and 141.6 cm^{-1} in the R2PI spectrum of 2PI shown in Fig. 2b. Therefore, the observed 41.1 cm^{-1} and 141.6 cm^{-1} fundamentals are assigned to the puckering and flapping modes of 2PI_{ax}, respectively. The drop in the frequencies of the puckering and flapping modes of 2PI-d₅ to 40.2 cm^{-1} and 139.9 cm^{-1} , respectively, is caused by the higher reduced masses of the modes in 2PI-d₅ than in 2PI. The relatively intense vibronic transition at $\sim 700\text{ cm}^{-1}$ in the spectra of indan derivatives is associated with the in-plane bending of indan ring [2, 3]. Similar transitions also appear in the spectra of 2PI and 2PI-d₅ at 730.1 cm^{-1} and 723.0 cm^{-1} , respectively. The combinations of these fundamentals with

the fundamentals of puckering mode appear at 771.2 and 762.8 cm^{-1} in the spectra of 2PI and 2PI-d₅, respectively.

Full deuteration of the phenyl ring of 2PI causes the electronic origin of 2PI-d₅ to blue-shift by only 0.4 cm^{-1} , suggesting that the $S_1 \leftarrow S_0$ transition of 2PI is localized on the indan chromophore. The biggest difference between the spectra of 2PI and 2PI-d₅ is associated with the peaks at 605.4 cm^{-1} and 773.1 cm^{-1} above the electronic origins of 2PI and 2PI-d₅, respectively. The two peaks are assigned to the electronic origins of the $S_2 \leftarrow S_0$ transitions of 2PI and 2PI-d₅ that are localized on the phenyl and phenyl-d₅ chromophores, respectively. The observed energy gap between the $S_2 \leftarrow S_0$ origins of 2PI and 2PI-d₅ is 167.7 cm^{-1} , which is close to the energy gap of 165.9 cm^{-1} between the electronic origins of toluene and toluene-d₅ [18]. The observation of localized $S_1 \leftarrow S_0$ and $S_2 \leftarrow S_0$ transitions of 2PI indicates that the phenyl and indan rings of 2PI are perpendicular to each other. According to the TDDFT/B3LYP/6-311G(d,p) calculations, the $S_1 \leftarrow S_0$ transition is mostly dominated by a single transition (with CI coefficient of 0.55) from HOMO to LUMO + 1 orbital. As seen in Fig. 3, these two orbitals are completely localized on the indan chromophore. The $S_2 \leftarrow S_0$ transition is dominated by two transitions: (HOMO-1 to LUMO with CI coefficient of 0.36) and (HOMO-1 to LUMO + 2 with CI coefficient of 0.36). Thus, the localized nature of the $S_1 \leftarrow S_0$ and $S_2 \leftarrow S_0$ transitions is supported by the TDDFT calculations.

Conformational relaxation of 2PI and 2MI

Very fast relaxation of the 2PI_{eq90} conformer to the more stable 2PI_{eq0} conformer is anticipated due to the very low

barrier of 0.06 kcal/mol to such transition (TS_{eq} in Scheme 3). Therefore, only two conformers ($2PI_{eq0}$ and $2PI_{ax}$) of 2PI are expected to be observed in the supersonic jet experiments. However, the most intriguing aspect of this study appears to be the absence of $2PI_{eq0}$ in the supersonic jet expansion. It has been observed that barriers to conformational interconversions in a supersonic jet can be surmounted if the barriers are less than $2kT$ [14]. Where k is the Boltzmann constant; T is the pre-expansion temperature (383 K for 2PI and 298 K for 2MI). The computed barrier to axial-equatorial interconversion in 2PI (TS_{ax-eq} in Scheme 3) is 1.68 kcal/mol above the $2PI_{eq0}$ local minimum. This barrier is about the same as $2kT$ (1.52 kcal/mol) of 2PI. Meanwhile, the barrier to axial-equatorial interconversion in 2MI (TS_{ax-eq} in Scheme 2) is 2.33 kcal/mol above the $2MI_{eq}$ minimum. Thus, the barrier in 2MI is substantially larger than $2kT$ (1.16 kcal/mol) of 2MI. The lower barrier in 2PI can be attributed to the higher stabilizing effect of the $C_{sp^2}-H/\pi$ interactions in the transition state of 2PI (TS_{ax-eq} in Scheme 3) than in the transition state of 2MI (TS_{ax-eq} in Scheme 2). Therefore, conformational relaxation of the equatorial isomers of 2PI occurs because of the high pre-expansion temperatures and relatively low barrier to axial-equatorial interconversion.

Conclusions

Both axial ($2MI_{ax}$) and equatorial ($2MI_{eq}$) conformers of 2MI have been observed. A $2MI_{eq}/2MI_{ax}$ conformer ratio of 2.3 was estimated at 298 K, leading to the energy difference, $\Delta E = E_{2MI_{ax}} - E_{2MI_{eq}}$, of 0.49 kcal/mol. Only the axial conformer of 2PI was observed in the supersonic jet expansion. The equatorial conformers of 2PI relax to the more stable axial conformer because of the high pre-expansion temperatures and relatively low barrier to axial-equatorial interconversion. The barrier to axial-equatorial interconversion in 2MI is high enough to prevent conformational relaxation at the pre-expansion temperature of 298 K. The results of this study show that intramolecular C–H/ π interactions are more important in determining the conformational stability of 2PI than 2MI. This can be attributed to the higher acidity of the $C_{sp^2}-H$ bond ($pK_a \sim 44$) than that of $C_{sp^3}-H$ bond ($pK_a \sim 50$). The $S_1 \leftarrow S_0$ and $S_2 \leftarrow S_0$ transitions of 2PI are found to be completely localized on the indan and phenyl chromophores, respectively, suggesting that the phenyl and indan rings of 2PI are perpendicular to each other.

Acknowledgments The author is grateful to Dr. John R. Cable, Bowling Green State University, Ohio, for providing the facility used for this research.

References

- Shibasaki K, Fujii A, Mikami N, Tsuzuki S (2007) J Phys Chem A 111:753
- Iga H, Isozaki T, Suzuki T, Ichimura T (2007) J Phys Chem A 111:5981
- Isozaki T, Iga H, Suzuki T, Ichimura T (2007) J Chem Phys 126:214304
- Tsuzuki S, Honda K, Uchimaru T, Mikami M, Fujii A (2006) J Phys Chem A 110:10163
- Zwier TS (1996) Annu Rev Phys Chem 47:205
- Al-Saadi AA, Wagner M, Laane J (2006) J Phys Chem A 110:12292
- Das A, Mahato KK, Panja SS, Chakraborty T (2003) J Chem Phys 119:2523
- Morita S, Fujii A, Mikami N, Tsuzuki S (2006) J Phys Chem A 110:10583
- Panja SS, Chakraborty T (2003) J Chem Phys 118:6200
- Hopkins JB, Powers DE, Smalley RE (1980) J Chem Phys 72:5039
- Im HS, Bernstein ER, Secor HV, Seeman JI (1991) J Am Chem Soc 113:4422
- Arp Z, Meinander N, Choo J, Laane J (2002) J Chem Phys 116:6648
- Barbu-Debus KL, Lahmani F, Zehnacker-Rentien A, Guchhait N, Panja SS, Chakraborty T (2006) J Chem Phys 125:174305
- Ottaviani P, Velinob B, Caminati W (2006) J Mol Struct 795:194
- Finley JP, Cable JR (1993) J Phys Chem 97:4595
- Frisch MJ, Trucks GW, Schlegel HB, Scuseria GE, Robb MA, Cheeseman JR, Montgomery JA JR, Vreven T, Kudin KN, Burant JC, Millam JM, Iyengar SS, Tomasi J, Barone V, Mennucci B, Cossi M, Scalmani G, Rega N, Petersson GA, Nakatsuji H, Hada M, Ehara M, Toyota K, Fukuda R, Hasegawa J, Ishida M, Nakajima T, Honda Y, Kitao O, Nakai H, Klene M, Li X, Knox JE, Hratchian HP, Cross JB, Adamo C, Jaramillo J, Gomperts R, Stratmann RE, Yazayev O, Austin AJ, Cammi R, Pomelli C, Ochterski JW, Ayala PY, Morokuma K, Voth GA, Salvador P, Dannenberg JJ, Zakrzewski VG, Dapprich S, Daniels AD, Strain MC, Farkas O, Malick DK, Rabuck AD, Raghavachari K, Foresman JB, Ortiz JV, Cui Q, Baboul AG, Clifford S, Cioslowski J, Stefanov BB, Liu G, Liashenko A, Piskorz P, Komaromi I, Martin RL, Fox DJ, Keith T, Al-Laham MA, Peng CY, Nanayakkara A, Challacombe M, Gill PMW, Johnson B, Chen W, Wong MW, Gonzalez C, Pople JA (2003) Gaussian 03, Revision B.03. Gaussian, Inc., Wallingford, CT
- Wiberg KB, Castejon H, Bailey WF, Ochterski J (2000) J Org Chem 65:1181
- Walter JB, Ram SR (1994) Can J Phys 72:1225
- Sotoyama W, Sato H, Matsuura A, Sawatari N (2006) J Mol Struct 759:165